Using electric propulsion for the de-orbiting of satellites

Application to sun-synchronous satellites

Christian M. Fromm, Armin Herbertz

Abstract According to the Space Debris Mitigation Guidelines satellites in Low Earth Orbit (hereafter LEO) should be removed with 25 years after its operational end-of-life. Especially satellites in a sun-synchronous orbit (hereafter SSO) represent a large thread for other satellites due to the rotation of their orbit induced by the oblateness of the Earth. Given the recent and future advances in electric propulsion systems, these engines have the potential to replace the typical chemical engines used for the de-orbiting manoeuvre. In this paper we use different electric propulsion systems and analyse their capability and applications for the de-orbiting of SSO-satellites.

1 Introduction

During the last decades the importance of satellites for the every day life has increased continuously, leading to an increase in the number of satellites deployed into space. Most of the satellites delivered into space are not removed from their operating orbit. Given the growing number of objects in space, especially in LEO, the possibility of collision with recent space debris (satellite or launcher fragments) increases. These collision could lead, depending on the size of the impact object to minor damages (no mission failure), to major damages (mission failure), to partial fragmentation (break up of satellite parts) or in the worst case to a total fragmentation of the satellite. The latter can easily produce up to 1000 fragments of various sizes from μm to m. Therefore, recent and future satellites should be transferred into an end-of-life orbit or should be de-orbited according to the Space Debris Mitigation Guidelines in order to decrease the amount of space debris and thus guarantee access to space for future generations [3].
Among the various possible orbits in LEO $(160\,\text{km} \leq h \leq 2400\,\text{km})$ the most interesting ones with respect to the avoidance of space debris are those with an inclination $i > 90^\circ$, the so-called SSO. Due to the oblateness of the Earth, the right ascension of the ascending node (hereafter Ω) increases and leads to a rotation of the orbit. Assuming a total fragmentation of a SSO satellite, its fragments will encounter different variations in their orbital elements due to the oblateness of the Earth and the atmospheric drag (see Sect. 2 for details). Therefore the fragmentation cloud will envelope the earth roughly 1 year after the collision, presenting a enormous thread for other objects in space ,see e.g., [7].
Given the recent and possible future advances in the field of electric propulsion together with the fact that a SSO satellite spend most of its orbital time in sunlight, we investigate in this paper the possibility and capability of electric engines for de-orbiting of SSO satellites.
The organisation of the paper is the following: In Sect. 2 we present the basic equations covering the orbit of satellites including perturbation forces of various origins and in Sect. 3 we use the derived relations to de-orbit a SSO satellites via different electric propulsion. We discussion our results in Sect. 4 and provide a summary in Sect. 5.

C. M. Fromm
DLR (German Aerospace Centre), Institute of Space Propulsion, 74239 Hardthausen, Germany
E-mail: christian.fromm@dlr.de
A. Herbertz
DLR (German Aerospace Centre), Institute of Space Propulsion, 74239 Hardthausen, Germany
E-mail: armin.herbertz@dlr.de

2 Theory

2.1 Orbital elements and perturbations

The orbit of a satellite can be described by six Keplerian elements, the semi-major axis, a, the eccentricity, e, the inclination, i, the right ascension of the ascending node, Ω, the argument of perigee, ω, and the true anomaly, θ. The latter is used to determine the position of the satellite within the orbit. Assuming a perfect spherical Earth and under the absence of perturbing forces, the orbit would be closed and fixed in space, i.e., no variation in the orbital elements, a, e, i, Ω and ω.

2.2 Perturbation Theory

As mentioned earlier, any perturbation acting on a satellite leads to a variation of its orbital elements. In this work we use the Gauss variational equations for the calculation of the perturbed orbital elements.

$$\frac{da}{dt} = \frac{2a^2}{h}\left(e\sin\theta a_\mathsf{r} + pr^{-1}a_\mathsf{t}\right) \tag{1}$$

$$\frac{de}{dt} = h^{-1}\left(p\sin\theta a_\mathsf{r} + \left([p+r]\cos\theta + re\right)a_\mathsf{t}\right) \tag{2}$$

$$\frac{di}{dt} = h^{-1}r\cos\left(\omega+\theta\right)a_\mathsf{n} \tag{3}$$

$$\frac{d\Omega}{dt} = \frac{r\sin\left(\omega+\theta\right)}{h\sin i}a_\mathsf{n} \tag{4}$$

$$\frac{d\omega}{dt} = -\frac{d\Omega}{dt}\cos i - \frac{1}{he}\left(p\cos\theta a_\mathsf{r} - (p+r)\sin\theta a_\mathsf{t}\right) \tag{5}$$

$$\frac{dE}{dt} = \frac{na}{r} + \frac{1}{nae}\left(\left[\cos\theta - e\right]a_\mathsf{r} - \left[1+\frac{r}{a}\right]\sin\theta a_\mathsf{t}\right), \tag{6}$$

where $p = a\left(1-e^2\right)$, $\sqrt{GM_\mathsf{e}p}$, $n = \sqrt{GM_\mathsf{e}a^{-3}}$, $r = p/(1+e\cos\theta)$ and E is the eccentric anomaly. In the equations above G corresponds to the gravitational constant, M_e to the mass of the Earth, and $a_{\mathsf{r,t,n}}$ to perturbing acceleration radial, transversal and normal i.e., perpendicular, to the orbital plane.

2.3 Oblateness of the Earth

For more realistic calculations of the motion of a satellite within the gravitational potential of the Earth, one has to take into the depart of the planet from spherical symmetry, caused, e.g., by its rotation. The gravitational potential of the Earth or any given planet can be expressed in terms of the Legendre polynomials. The resulting perturbing acceleration can be written as:

$$a_{\mathsf{r,J2}} = -\frac{GM_e}{r^2}\frac{3}{2}J_2\left(\frac{R_e}{r}\right)^2\left[1-3\sin^2 i\sin^2(\omega+\theta)\right] \tag{7}$$

$$a_{\mathsf{t,J2}} = -\frac{GM_e}{r^2}\frac{3}{2}J_2\left(\frac{R_e}{r}\right)^2\sin^2 i\sin\left[2(\omega+\theta)\right] \tag{8}$$

$$a_{\mathsf{n,J2}} = -\frac{GM_e}{r^2}\frac{3}{2}J_2\left(\frac{R_e}{r}\right)^2\sin 2i\sin(\omega+\theta), \tag{9}$$

where M_e and R_e are the mass and radius of the Earth and $J_2 = 0.00108263$ is the Jeffery's constant of second order (see e.g., [1]). Inserting the equations above into Eqs. 1 to 5 and performing an integration over one orbital period leads to the well known results for the non-vanishing orbital elements $d\Omega/dt$ and $d\omega/dt$:

$$\frac{d\Omega}{dt} = -\left[\frac{3}{2}\frac{\sqrt{GM_e}J_2R_e^2}{\left(1-e^2\right)^2a^{7/2}}\right]\cos i \tag{10}$$

$$\frac{d\omega}{dt} = -\left[\frac{3}{2}\frac{\sqrt{GM_e}J_2R_e^2}{\left(1-e^2\right)^2a^{7/2}}\right]\left(\frac{5}{2}\sin^2 i - 2\right) \tag{11}$$

As can be seen from the equations above, the oblateness of the Earth leads to a continuous increase in Ω and ω and thus to a rotation of the orbital plane.

2.4 The atmosphere of the Earth

The next perturbation force we take into account in the simulations is the drag induced due to the motion of the satellite in the atmosphere of the Earth. For reasons of simplicity we use US--standard atmosphere neglecting the influence of the sun activity on the density and composition of the upper layers of the atmosphere. In future works we plane to include an atmospheric model using TD88 or NASAs' NRLMSISE-00. Assuming that the atmosphere is co-rotating with the Earth, the perturbing acceleration acting on a satellite can be approximated by:

$$a_{\mathrm{r,atmos}} = -\frac{1}{2} K_{\mathrm{D}} \rho v \sqrt{\frac{GM_e}{p}} e \sin\theta \tag{12}$$

$$a_{\mathrm{t,atmos}} = -\frac{1}{2} K_{\mathrm{D}} \rho v \left(\sqrt{\frac{GM_e}{p}} \frac{p}{r} - \sigma r \cos i \right) \tag{13}$$

$$a_{\mathrm{n,atmos}} = -\frac{1}{2} K_{\mathrm{D}} \rho v \sigma r \sin i \cos(\theta + \omega), \tag{14}$$

where ρ is the altitude dependent density and $K_{\mathrm{D}} = C_{\mathrm{D}} \frac{A}{m} \sqrt{k_r}$ with drag coefficient C_{D}, surface A, mass m, velocity $v = \sqrt{2(GM_e/r - GM_e/(2a))}$ and k_r is given by:

$$k_r \approx 1 - \frac{2\sigma h \cos i}{v^2}, \tag{15}$$

with $\sigma = 7.292 \cdot 10^{-5}$rad/s and angular momentum $h = \sqrt{GM_e a(1-e^2)}$. The impact of the atmospheric drag on the orbital elements can be obtained by inserting Eqs. 12 -14 into the perturbation equations (Eqs. 1 to 5). The main effect of the atmospheric drag on the orbital elements can be summarised as follows: Due to the $-$ sign in Eqs. 12 - 14 the semi-major axis a decreases and the eccentricity approaches $e = 0$ with minor effects on the other orbital elements.

2.5 Low thrust acceleration

Since the perturbation forces induced on the satellite due to the oblateness and the atmosphere of the Earth are not sufficiently large enough to de-orbit a satellite above a certain altitude ($h \sim 120\,$km) within the required time span of 25 years, we need to use an additional acceleration provided by a propulsion system. In general, the acceleration provided by the propulsion system can be written as:

$$a_{\mathrm{r,thrust}} = \frac{F_{\mathrm{t}}}{m} \sin\alpha \cos\beta \tag{16}$$

$$a_{\mathrm{t,thrust}} = \frac{F_{\mathrm{t}}}{m} \cos\alpha \cos\beta \tag{17}$$

$$a_{\mathrm{n,thrust}} = \frac{F_{\mathrm{t}}}{m} \sin\beta\ , \tag{18}$$

with α and β the pitch (in-plane) and yaw (out off-plane) steering angles and F_{t} the thrust provided by the selected propulsion system. The fuel consumed by the propulsion system is computed in the case of an electric engine by:

$$\frac{dm}{dt} = -\frac{2\eta P}{(g I_{\mathrm{sp}})^2}, \tag{19}$$

where η is efficiency, P the required power of the system, $g = 9.81\,\mathrm{m/s^2}$ the gravitational acceleration on the surface of the Earth, and I_{sp} the specific impulse of the system. In order to track the fuel consumption during the de-orbiting, the equation above is include in the set of differential equation given in Eqs. 1 - 5.

2.6 Shadow phases

Since we are using an electric propulsion system for the de-orbiting we have to take into account possible eclipsing phases which could occur during the manoeuvre. Within the simulation we do not distinguish between umbra and penumbra. Since the system does not provide thrust during the eclipses we need to know the position where the satellite enters and leaves the shadow of the Earth. The entry and exit position depend

on the position of the satellite relative to the Sun and to the Earth. If we assume a conical shadow geometry, the shadow function can be written as:

$$s_c = \frac{\mathbf{r}_{\text{sat}} \cdot \mathbf{r}_{\text{sun}}}{r_{\text{sun}}} + \cos\beta \left[\sqrt{r_{\text{sat}} - R_e^2 \cos\beta^2} - R_e \sin\beta \right], \tag{20}$$

where $\mathbf{r}_{\text{sat,sun}}$ is the position vector of the satellite and the Sun in the geo-centric coordinate system respectively, and $\beta = \arctan\left(R_e + R_s\right) / \left|\mathbf{r}_{\text{sat}} - \mathbf{r}_{\text{sun}}\right|$ with R_s the radius of the Sun. If $s_c \leq 0$ the satellite is the shadow and in the sunlight for $s_c > 0$. Given the orbital elements of the satellite together with the starting date, the shadow entry and exit position can be computed (see Fig. 1).

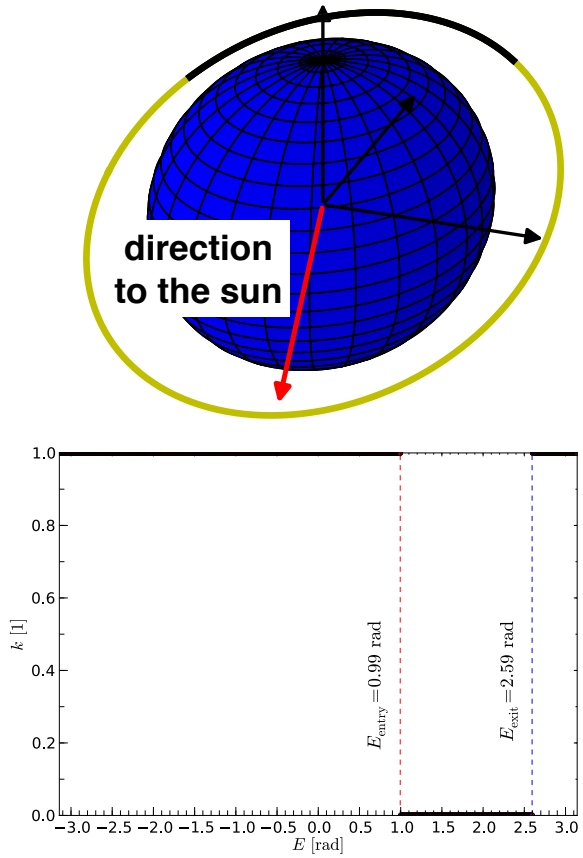

Fig. 1 Results of the shadow calculation for a satellite orbit with $a = 8900$ km, $i = 28°$ and $e = \Omega = \omega = 0$. Top: 3d representation of the orbit. The red arrow corresponds to the direction of the sun. The yellow part of the orbit indicates the position where the satellite is in the sun light and black part the position where the satellite is in the shadow of the Earth. Bottom: Shadow function, k, as function of the eccentric anomaly, E. The eccentric anomaly at shadow entry and shadow exit are indicated by the dashed vertical lines and the shadow function, k, is set to zero during the shadow phase.

2.7 Orbital averaging technique

Since we are mainly interested in the total time and fuel required to de-orbit a SSO satellite, we use the technique of orbital averaging to accelerate the calculations. Therefore, we re-write the differential equations given in Eqs. 1 to 5 in terms of the eccentric anomaly E using $dE/dt \sim na/r$ assuming that the second term in Eq. 6 can be neglected. This leads to a new set of differential equations:

$$\frac{da}{dE} = \frac{2a^3}{GM_e}\left(e\sin E a_\mathsf{r} + \sqrt{1-e^2}a_\mathsf{t}\right) \tag{21}$$

$$\frac{de}{dE} = \frac{a^2}{GM_e}\Big[\sin E\left(1-e^2\right)a_\mathsf{r} + \left(2\cos E - e - e\cos^2(E)\right)\sqrt{(1-e^2)}a_\mathsf{t}\Big] \tag{22}$$

$$\frac{di}{dE} = \frac{a^2}{GM_e}\left[\frac{\cos\omega\cos E - e\cos\omega}{\sqrt{1-e^2}} - \sin\omega\sin E\right](1-e\cos E)\,a_\mathsf{n} \tag{23}$$

$$\frac{d\Omega}{dE} = \frac{a^2}{GM_e}\left[\frac{\sin\omega\cos E - e\sin\omega}{\sqrt{1-e^2}} + \cos\omega\sin E\right]\frac{1-e\cos E}{\sin i}a_\mathsf{n} \tag{24}$$

$$\frac{d\omega}{dE} = -\cos i\frac{d\Omega}{dE} - \frac{a^2}{eGM_e}\Big[(\cos E - e)\sqrt{1-e^2}a_\mathsf{r} + \left(2-e^2-e\cos E\right)\sin(E)a_\mathsf{t}\Big] \tag{25}$$

$$\frac{dm}{dE} = -\frac{2\eta P}{\left(gI_\mathsf{sp}\right)^2}\frac{r}{na} \tag{26}$$

The equations above are integrated for one orbit, i.e. $-\pi \leq E \leq \pi$ or adequate integration boundaries taking the eclipsing phases into account. The mean changes in the orbital elements during one revolution can be computed as:

$$\dot{\mathbf{x}} = \frac{1}{T_p}\int_{E_1}^{E_2}\frac{d\mathbf{x}}{dE}dE, \tag{27}$$

where $\mathbf{x} = [a, e, i, \Omega, \omega, m]^T$ is the state vector and $T_p = 2\pi a^{3/2}/\sqrt{GM_e}$ is the orbital period and $E_{1,2}$ is the lower and upper integration boundary. As long as the difference between orbital averaged and time integrated changes in the orbital elements are small, the averaged changes can be propagated in time. Here we use typical time span of $\Delta t \sim 5$ days, before we update the average changes in the orbital elements using Eqs. 21 to 26 together with an updated state vector.

2.8 Steering laws and trajectory optimisation

In order to obtain the optimal de-orbiting manoeuvre using a direct optimisation approach we have to parameterize the thrust steering direction. The thrust steering direction is given by:

$$\mathbf{u} = \left[\sin\alpha\cos\beta, \cos\alpha\cos\beta, \sin\beta\right]^T, \tag{28}$$

(see also Eqs 16 to 18) and is characterised by the pitch, α, and the yaw, β, steering angles. The major aim of the de-orbiting is to lower the semi-major axis a while reducing the eccentricity, e, and if possible the inclination, i. For this purpose, we can define a Hamiltonian function (see, e.g.,[2]):

$$\mathcal{H}\left(\mathbf{x}, \mathbf{u}, \boldsymbol{\lambda}\right) = \lambda_a\frac{da}{dE} + \lambda_e\frac{de}{dE} + \lambda_i\frac{di}{dE}, \tag{29}$$

with costate variables $\boldsymbol{\lambda} = [\lambda_a, \lambda_e, \lambda_i]^T$. The pitch and yaw steering laws can be obtained from the Hamiltonian function by computing its derivation with respect to α ($\partial\mathcal{H}/\partial\alpha$) and β ($\partial\mathcal{H}/\partial\beta$). After some mathematical

manipulations the following steering laws are derived:

$$\sin\alpha = \frac{-B/A}{\sqrt{1+(B/A)^2}} \tag{30}$$

$$\cos\alpha = \frac{1}{\sqrt{1+(B/A)^2}} \tag{31}$$

$$\sin\beta = \frac{\left(\lambda_a C + \lambda_e D\right)/\lambda_i E}{\sqrt{1+\left(\frac{\lambda_a C+\lambda_e D}{\lambda_i E}\right)^2}} \tag{32}$$

$$\cos\beta = \frac{1}{\sqrt{1+\left(\frac{\lambda_a C+\lambda_e D}{\lambda_i E}\right)^2}}, \tag{33}$$

where A, B, C, D, and E are functions of the orbital elements and are given by:

$$A = 2\lambda_a a e \sin E + \lambda_e\left(1-e^2\right)\sin E \tag{34}$$

$$B = \sqrt{1-e^2}\left[2\lambda_a a - \lambda_e\left(2\cos E - e - e\cos^2 E\right)\right] \tag{35}$$

$$C = 2a\left(e\sin E\sin\alpha + \sqrt{1-e^2}\cos\alpha\right) \tag{36}$$

$$D = \left(1-e^2\right)\sin E\sin\alpha + \left(2\cos E - e - e\cos^2 E\right)\sqrt{1-e^2}\cos\alpha \tag{37}$$

$$E = \left[\frac{\cos\omega\cos E - e\cos\omega}{\sqrt{1-e^2}} - \sin\omega\sin E\right](1-e\cos E) \tag{38}$$

Following [2] it is meaningful to parameterize the costate variables along the semi-major axis by several grid points and to perform a linear interpolation between them.
For the optimisation we search for the optimal steering law which minimises the select performance index J which is subject to the equations of motion, $\dot{\mathbf{x}} = f(t, \mathbf{x}, \mathbf{u})$ i.e., the variation in the orbital elements due to several perturbations, and to the final state constraints $\psi\left[\mathbf{x}\left(t_f\right), t_f\right]$. For this purpose we use a parallel Lagrange multiplier particle swarm optimizer [4].

3 Results

3.1 Simulation setup

For the simulations we use a generic SSO-satellite with an initial mass of $m = 8200\,\text{kg}$. The orbital elements and other characteristic values of the satellite are summarised in Table 1.

Table 1 Initial orbital elements and geometry used for the SSO-satellite

orbital element	value
semi-major axis	$a = 7200\,\text{km}$
eccentricity	$e = 1 \cdot 10^{-3}$
inclination	$i = 98.5°$
RAAN	$\Omega = 0.0°$
argument of perigee	$\omega = 0.0°$
mass	$m = 8200\,\text{kg}$
surface	$A = 50\,\text{m}^2$
drag coefficient	$C_\text{D} = 2.0$

The time a satellite would stay in space without active de-orbiting can be computed using the acceleration induced by atmosphere (Eqs. 12 - 14) and inserting them into the Gauss variational equations (Eqs. 21 to 25). The results for the life time of the SSO-satellite using the parameters presented in Table 1 can be seen in Fig. 2.

The time required to lower the altitude of the satellite to $h \sim 150\,\text{km}$ is in the order of 150 years. This results stresses the necessity of a propulsion system in order to remove a SSO-satellites within 25 years as

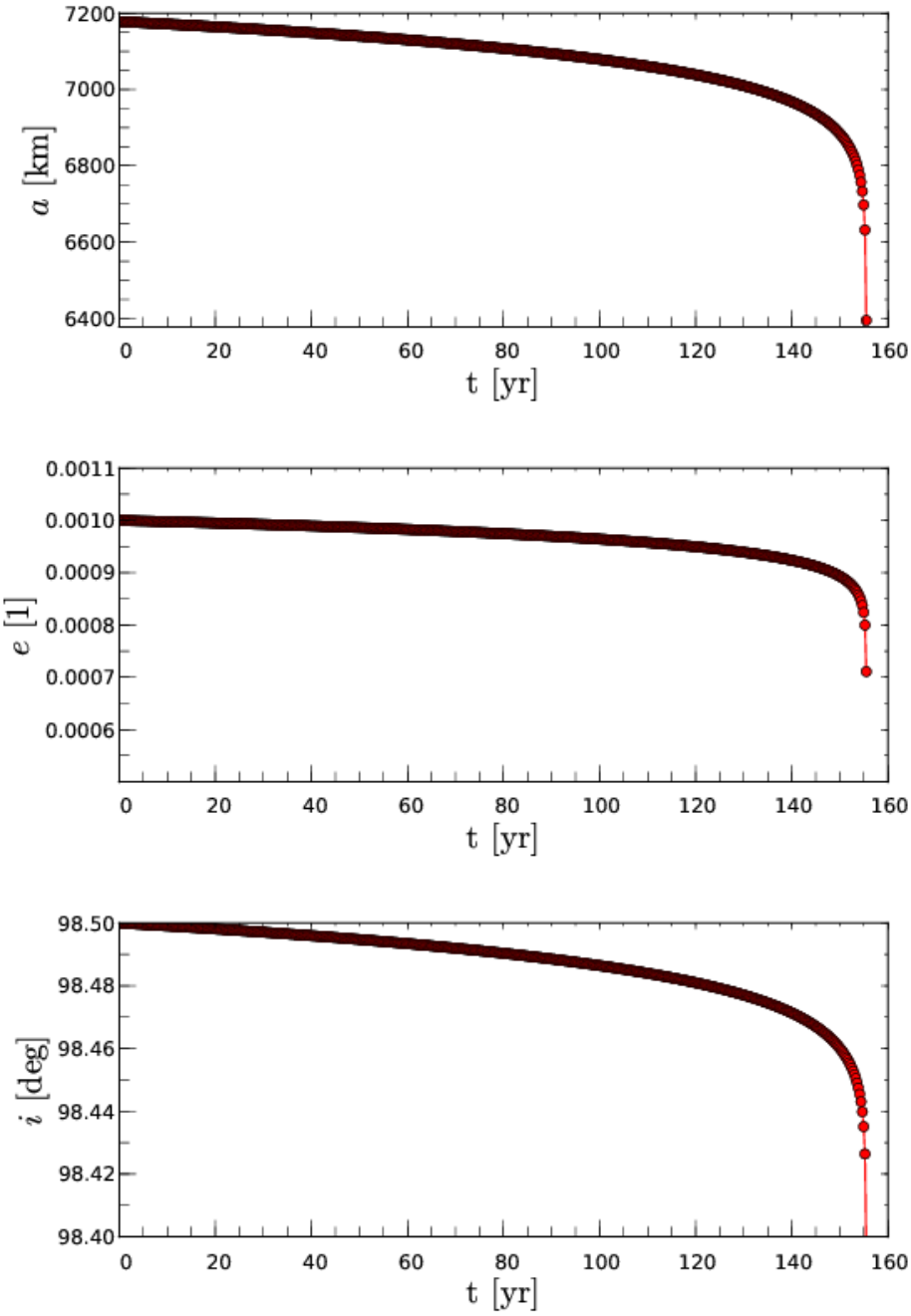

Fig. 2 The variation of the orbital elements of a SSO-Satellite (see Table 1 for initial orbital elements) due to the atmosphere of the Earth. From top to bottom, the time evolution of the semi-major axis, a, the eccentricity, e, and inclination, i. Notice, that the x-axis is plotted in years.

recommended by the Space Debris Mitigation Guidelines [3].

For the electric propulsion we selected eight different systems and their typical parameters are listed in Table 2. In all simulations we set the final altitude to $h \sim 150\,\text{km}$ which corresponds to a semi-major axis of $a \sim 6500\,\text{km}$. Additionally, we restrict the eccentricity $e \leq 1 \cdot 10^{-3}$ and the inclination $i \leq 98.5°$. In Fig. 3 we show the de-orbiting of the SSO-satellite using the RIT-XT Ion Thruster. The panels show the variation of the semi-major axis (top) and the mass of the satellite i.e., the consumed fuel (bottom). The used costate variables during the de-orbit manoeuvre as function of the semi-major axis are plotted in Fig. 4.

Table 2 Used electric propulsion systems

name	typ	I_{sp} [s]	F_t [mN]	P [W]	η [%]
RIT-4	Ion	4660	3.2	115	24.5
DS4G	Ion	14000	5.0	450	15.0
μ10	Ion	3200	8.0	348	36.0
RIT-10	Ion	3398	10	340	53.0
UK10	Ion	3300	23	700	55.0
RIT-XT	Ion	4600	120	3260	60.0
RIT-22	Ion	4200	200	7000	71.5
NEXIS	Ion	7500	473	20000	76.0

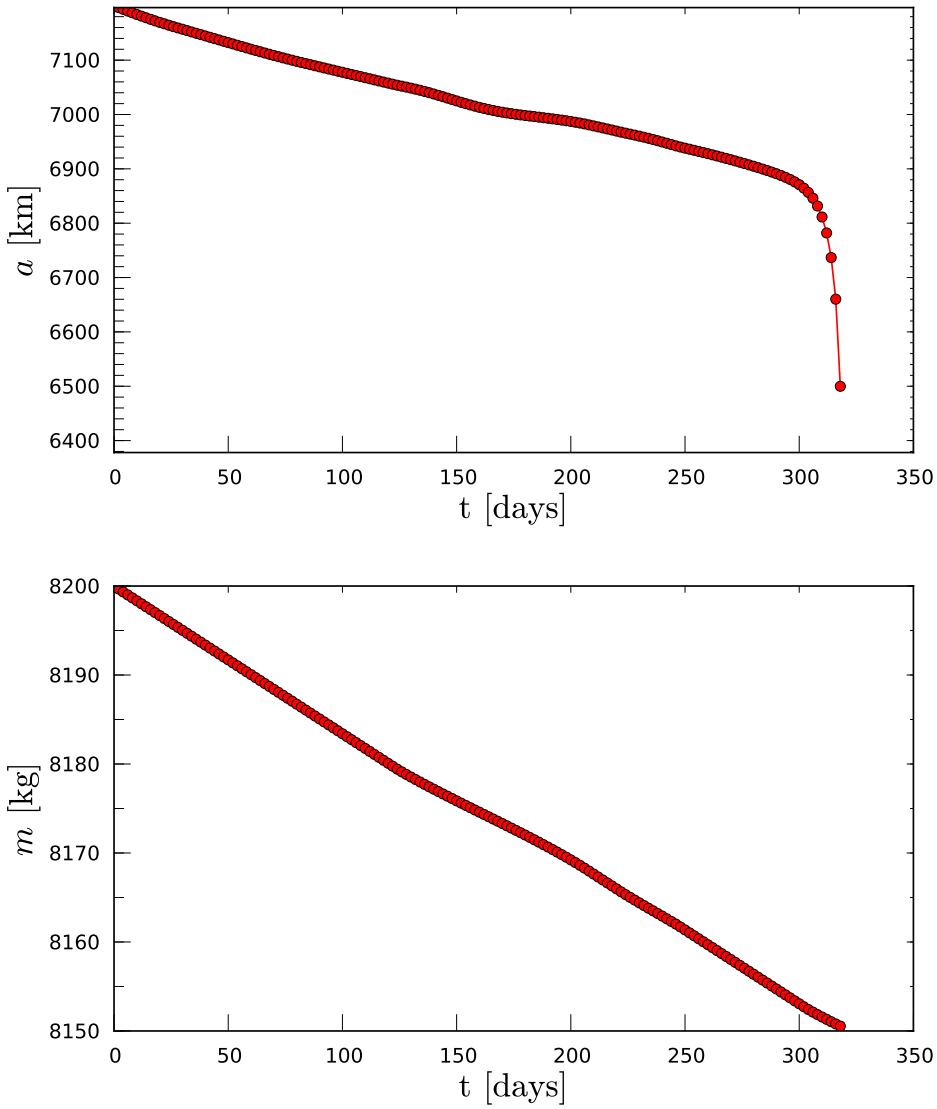

Fig. 3 The temporal variation of the semi-major axis, a, (top) and the mass, m, of the satellite, i.e., the used fuel (bottom) during the de-orbiting of the SSO-satellite using the RIT-XT Ion Thruster.

The time required for the de-orbiting of a SSO-satellite (see Table 1 for initial data) depends strongly on the thrust provided by the system, whereas the consumed fuel additionally depends on the type of the propulsion system. In Table 3 we present the required time and fuel for the de-orbiting of the SSO satellite together with the size of the solar arrays and their mass. For the calculation of the solar array size we use XTJ Solar Cells from Spectro Lab, a triple junction solar cell with an efficiency of $\eta = 29.5\%$ [6]. The required

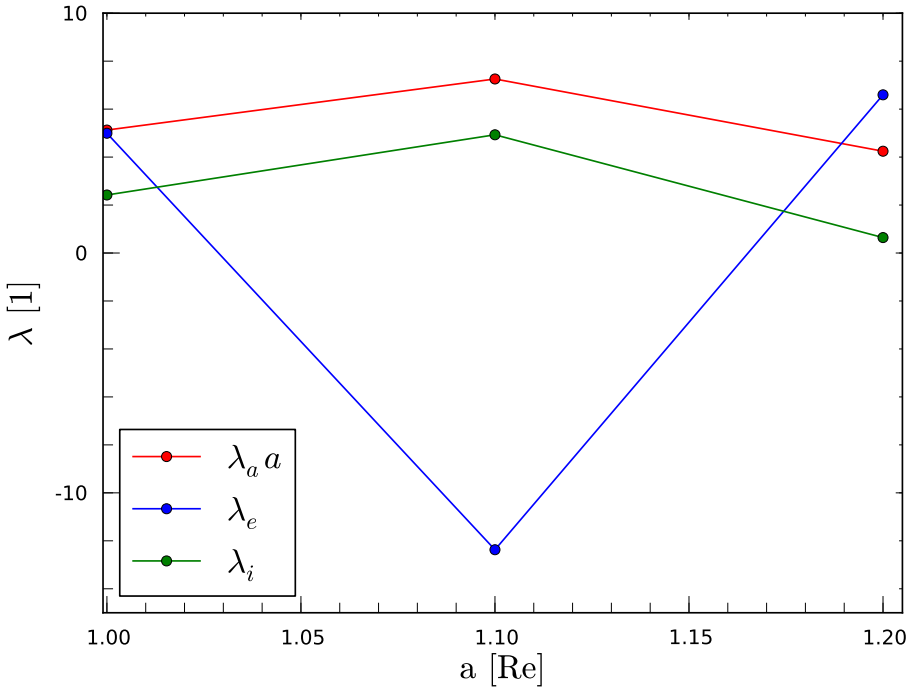

Fig. 4 Costate variables during the de-orbit of the SSO-satellite using the RIT-XT Ion Thruster.

size of the solar arrays can be computed by:

$$A = \frac{P_{\text{el}}}{H\eta}, \tag{39}$$

where we assume no degradation of the solar cells during the operation of the satellite and the de-orbiting[1], P_{el} is the power required by the propulsion system, H is the solar constant of 1367 W/m^2 and η is the efficiency of the solar cell.

Table 3 Results for the de-orbiting using different electric propulsion systems

name	t_{f} [days]*	m_{f} [kg]	$A^{\star}_{\text{sa}}$ [m^2]	$m^{\dagger}_{\text{sa}}$ [kg]
RIT-4	12529 (34.3)	23	0.3	0.5
DS4G	8019 (21.96)	4.0	2.2	3.7
μ10	5164 (14.14)	89	0.7	1.2
RIT-10	4164 (11.4)	93	0.9	1.5
UK10	1712 (4.69)	100	0.9	1.5
RIT-XT	318 (0.9)	49	8.1	13.6
RIT-22	192 (0.5)	88	17.4	29.2
NEXIS	80 (0.2)	38	49.6	83.2

* values in brackets correspond to the time in years
* assuming XTJ Solar Cells ($\eta = 29.5\%$) without significant solar panel degradation during operation
† using 0.84kg/m^2 and a cover glass with thickness of t=0.335 mm and a density of $\rho = 2.5$ g/cm^3

4 Discussion

The results of our calculations show that, expect for the RIT-4 system, it is possible to de-orbit a SSO satellite via an electric propulsion system within 25 years. However, the required time for the de-orbiting depends strongly on the thrust provided by the system and is decreasing with increasing thrust. The fuel required by the Ion Thrusters varies between 4 kg and 100 kg. These values have to be compared with typical fuel masses

[1] this assumption is only valid for satellites in LEO and for solar cells with cover glass thickness $t = 0.335$ mm

required by chemical propulsion systems. The velocity required to remove a satellite from a circular orbit into an elliptical orbit is given as:

$$\Delta v = v_{\mathsf{i}} \left(1 \sqrt{\frac{2\left(\tilde{a}-1\right)}{\left(\frac{\tilde{a}}{\cos\gamma_{\mathsf{f}}}\right)^2 - 1}} \right), \tag{40}$$

with initial velocity $v_{\mathsf{i}} = \sqrt{(GM_{\mathsf{e}})/a_i}$, $\tilde{a} = a_{\mathsf{i}}/a_{\mathsf{f}}$ is the ratio between the initial and final semi-major axis, and γ_{f} is the final flight path angle [5]. The propellant mass required to provide the velocity computed via Eq. 40 depends on the specific impulse, I_{sp}, of the propulsion system:

$$\Delta m = m \left[1 - \exp\left(-\frac{\Delta v}{I_{\mathsf{sp}} g_0} \right) \right]. \tag{41}$$

For the chemical de-orbiting we use a hydrazine thruster with a thrust of $F_{\mathsf{t}} = 400\,\mathsf{N}$ ($I_{\mathsf{sp}} = 224\,\mathsf{s}$). Given these engine settings and the orbital elements of the SSO satellite (see Table 1) we obtain a required propellant mass of $m_{\mathsf{f}} = 710\,\mathsf{kg}$. Given an Ion Thruster as propulsion system, the required fuel mass varies between $\left(5 \cdot 10^{-3} - 0.14\right) m_{\mathsf{f}}$ depending on the thrust of the system, making electric prolusion systems the perfect engine for the de-orbiting of SSO and LEO satellites.

5 Summary and Conclusion

In this paper we simulate the de-orbiting of a SSO satellite via electric propulsion taking into account the low-thrust nature of the propulsion system as well as the atmosphere and the oblateness of the Earth. Due to the used electric propulsion system we additionally consider shadow phases which occur during the propagation of the satellite.

In order to evaluate capability of electric propulsion systems we considered in our simulations Ion Thruster as well as Arcjet engines with different characteristic values. Our results show that an electric propulsion system with more than $F_t \geq 5\,\mathsf{mN}$ is able to remove the SSO satellite within the required 25 years as recommended by the Space Debris Mitigation Guidelines. Furthermore, the use of Ion Thrusters as propulsion system is favoured due to small fuel consumption during the de-orbiting.

Based on the results of the simulations the most promising electric propulsion system for the de-orbiting of a SSO-satellite (see Table 1), with respect to the consumed fuel, to the de-orbiting time and to the solar array size, should have a thrust between $100\,\mathsf{mN} \leq F_{\mathsf{t}} \leq 200\,\mathsf{mN}$. Such systems provide enough thrust to remove the Satellite within 1 year, do not require large solar arrays $A \sim 20\,\mathsf{m}^2$ and consume around $90\,\mathsf{kg}$ fuel.

References

1. Curtis, H. D., Orbital Mechanics for Engineering Students, Butterworth Heinemann, Oxford, (2013)
2. Conway, B. A., Spacecraft Trajectory Optimization, Cambridge University Press, New York, (2014)
3. IADC Space Debris Mitigation Guidelines, IDAC-02-01, 2002
4. Jansen P. and Perez R., Constrained Structural Design Optimization via a Parallel Augmented Lagrangian Particle Swarm Optimization, Journal of Computer and Structure, Vol 89 (13-14), 1352-1366 (2011)
5. Milstead, A. H., Deboost from Circular Orbits, The Journal of the Astronautical Sciences, Vol 13 (4), 170--171 (1966)
6. SpectroLab, XTJ 29.5% Next, Sylmar (CA), USA, (2014)
7. Wiedemann, C. and Braun, V. The Necessity of Removing a Sun-Synchronous Satellite, DGLR Conference (63), Augsburg (2014)